A Statistical Study of Easterly Waves in the Western Pacific: July–December 1964[1]

C.-P. CHANG, V. F. MORRIS AND J. M. WALLACE

Dept. of Atmospheric Sciences, University of Washington, Seattle

(Manuscript received 12 November 1969, in revised form 17 December 1969)

ABSTRACT

The period July–December 1964 in the tropical western Pacific was marked by strong fluctuations in the meridional wind component with periods ranging from 4–6 days. This paper describes an intensive study of these disturbances, using spectrum-analysis techniques on time series of radiosonde data.

Two types of disturbances appear to be involved. One of these, prevalent at Canton Island, is characterized by upward phase propagation in the lower troposphere and downward phase propagation above 200 mb. It has previously been suggested that this wave may be the tropospheric manifestation of the mixed Rossby-gravity wave. A second type of disturbance, prevalent at stations further west, is marked by an absence of vertical phase propagation. Latent heat release may be important in its energetics.

1. Introduction

In a recent issue of this journal Wallace and Chang (1969) [hereafter referred to as (A)] presented a statistical description of lower tropospheric wave disturbances in the tropics during the period July–December 1963. The present work is an extension of that study, using data for stations in the western Pacific during the period July–December 1964, a time of unusually intense wave activity in the period range of 4–5 days.

2. Data and procedures of analysis

The upper air data used in this study were taken from a selection of stations available in card deck No. 645 from the National Weather Records Center at Asheville, N. C. The procedures of analysis are similar to those used in (A). A list of stations with identifiers is given in Table 1. The period of record extends from July–December 1964.

A high-pass filter was applied to all the time series, except those for the meridional wind component, in order to remove long-term trends. The filter has a frequency response of $\sim 80\%$ at 30 days and $\geq 99\%$ for all periods ≤ 18 days. It has no significant effect on disturbances having the range of periods with which we will be concerned. The filter reduced the period of record from 6 months to 136 days extending from 25 July–7 December 1964.

The significance levels for the coherence data were extracted from a table prepared by J. M. Mitchell, Jr.,[2] based on data given in Amos and Koopmans (1963). One enters the table with the number of degrees of freedom of the coherence estimates. This is given by $1.25\ N/M$ where N is the number of data points (272) and M is the number of lags.

As in (A) we made extensive use of vertical averages in analyzing the data, wherever it could be justified. This made it possible to keep the number of time series within manageable limits, while retaining most of the relevant information contained in the data for many individual levels. The intervals for the vertical averaging were selected on the basis of interlevel cross-spectrum analysis.

Interlevel cross-spectrum analysis was performed on the time series for the meridional wind component v at each of the stations, using a 25-day lag period and 600 mb as the reference level. Coherence squares and phase differences between other levels and 600 mb were computed from the co- and quadrature-spectral estimates, summed over the 0.20, 0.22, 0.24 and 0.26 cycle per day frequency bands. When the smoothing of the spectral estimates is taken into account, it is found

TABLE 1. List of stations.

Station	Latitude	Longitude	WMO No.	Alphabetical identifier
Canton	3S	172W	91 700	C
Majuro	7N	171E	91 376	M
Kwajalein	9N	168E	91 366	J
Ponape	7N	134E	91 348	P
Truk	7N	151E	91 334	T
Guam	14N	144E	91 217	G
Yap	9N	138E	91 413	Y
Koror	7N	134E	91 408	K

[1] Contribution No. 216, Department of Atmospheric Sciences, University of Washington.

[2] Environmental Data Service, ESSA, Silver Spring, Md.

TABLE 2. Interlevel cross spectra.

a. Coherence square between v component at 600 mb and other levels for the 0.24 cycle day^{-1} frequency band.

(Significance level $\geq 95\%$ if coherence square ≥ 0.17.)

Station	Level (mb) sfc	850	700	500	450	400	350	300	250	200	175	150	125	100
Canton	0.54	0.40	0.53	0.56	0.53	0.17	0.12	0.20	0.49	0.60	0.40	0.29	0.33	0.55
Majuro	0.16	0.38	0.42	0.33	0.30	0.28	0.21	0.08	0.03	0.06	0.07	0.11	0.15	0.11
Kwajalein	0.24	0.26	0.63	0.77	0.66	0.48	0.43	0.40	0.30	0.30	0.33	0.23	0.35	0.13
Ponape	0.23	0.42	0.64	0.66	0.64	0.59	0.53	0.30	0.03	0.04	0.17	0.03	0.00	0.11
Truk	0.59	0.74	0.79	0.83	0.70	0.34	0.36	0.06	0.13	0.26	0.33	0.40	0.17	0.21
Guam	0.15	0.34	0.81	0.81	0.74	0.55	0.43	0.32	0.22	0.04	0.01	0.00	0.04	0.14
Yap	0.33	0.58	0.68	0.74	0.39	0.41	0.25	0.11	0.11	0.17	0.30	0.30	0.20	0.03
Koror	0.06	0.38	0.65	0.83	0.75	0.68	0.61	0.18	0.04	0.04	0.17	0.17	0.23	0.15

b. Phase difference (in cycles) between v component at 600 mb and other levels for the 0.24 cycle day^{-1} frequency band.

(Positive values indicate that 600-mb series leads the other series.)

Station	Level (mb) sfc	850	700	500	450	400	350	300	250	200	175	150	125	100
Canton	−0.40	−0.28	−0.10	0.13	0.10	0.06	—	0.21	0.29	0.29	0.31	0.28	0.18	0.06
Majuro	—	−0.13	−0.11	−0.01	0.05	0.07	0.09	—	—	—	—	—	—	—
Kwajalein	−0.15	−0.01	−0.01	0.04	0.05	0.07	0.08	0.05	−0.01	−0.01	−0.01	0.04	0.08	—
Ponape	−0.12	−0.05	−0.04	0.03	0.04	0.03	0.06	0.07	—	—	−0.40	—	—	—
Truk	−0.09	−0.08	−0.06	0.02	0.04	0.05	0.06	—	—	−0.43	−0.45	−0.48	0.45	0.11
Guam	—	−0.06	−0.01	−0.01	−0.03	−0.05	−0.06	−0.09	−0.11	−0.18	—	—	—	—
Yap	0.07	0.01	0.01	0.01	−0.03	−0.03	0.05	—	—	−0.32	−0.40	−0.38	−0.33	—
Koror	—	0.06	0.01	−0.03	−0.03	−0.02	0.02	0.08	—	—	−0.47	−0.43	−0.37	—

that the combined estimates possess ~17 degrees of freedom, which means that the coherence squares are $\geq 95\%$ significant if they are ≥ 0.17.

3. Results

The results of these computations are shown in Tables 2a, b. Phases are tabulated in cycles with positive values indicating that the 600-mb series leads the other series. The stations are arranged according to longitude, from east to west. At Canton Island, the easternmost station, the waves are distinctly upward propagating throughout the lower and middle troposphere, with $\frac{2}{3}$ of a cycle phase shift between the surface and 200 mb. There is a tendency for downward propagation above the 200-mb level, where the waves still maintain significant coherence with those at 600 mb. There is a distinct coherence minimum at ~350 mb and an upper level maximum at ~200 mb. Yanai *et al.* (1968) noticed a similar pattern data for Christmas Island during the spring of 1962.

West of Canton Island the vertical structure of the disturbances undergoes a marked change. In the lower troposphere the upward propagation is much less pronounced at the Marshall Island stations, and virtually nonexistent west of there. The relation between upper and lower tropospheric disturbances is rather confusing at the Marshall Island stations. At Majuro there appears to be little or no relation between upper and lower tropospheric waves while at Kwajalein there are indications that the waves are close to being in phase at all levels. West of the Marshalls the picture is more consistent. Ponape, Truk, Koror and Yap all show evidence of an abrupt phase change around the 300-mb level with the waves in the upper troposphere ~$\frac{1}{2}$ of a cycle out of phase with those in the lower troposphere. This is suggestive of equivalent barotropic disturbances which are "warm core" in the middle troposphere such that low-level troughs or cyclones are surmounted by upper level ridges or anticyclones.

TABLE 3. Scheme for vertical averaging.

Parameter	Symbol	Levels averaged
Zonal wind component	u_L	sfc, 950, 900, . . . 450, 400 mb
Meridional wind component	v_L	sfc, 950, 900, . . . 450, 400 mb
	v_H	200, 175, 150, 125 mb
Temperature	T_1	sfc, 950, 900 mb
	T_2	450, 400, . . . 250, 200 mb
	T_3	125 mb
Relative humidity	$\overline{RH}$	sfc, 950, 900, . . . 500, 550 mb

a. Spectra of the vertically averaged series

The above results suggest a simple scheme for vertical averaging which should be applicable to all stations except Canton Island. This scheme is outlined in Table 3. The wind fluctuations are divided into upper and lower layers in which they have opposing phase at the western stations. The temperature fluctuations are divided into three layers: T_1, below 900 mb where the

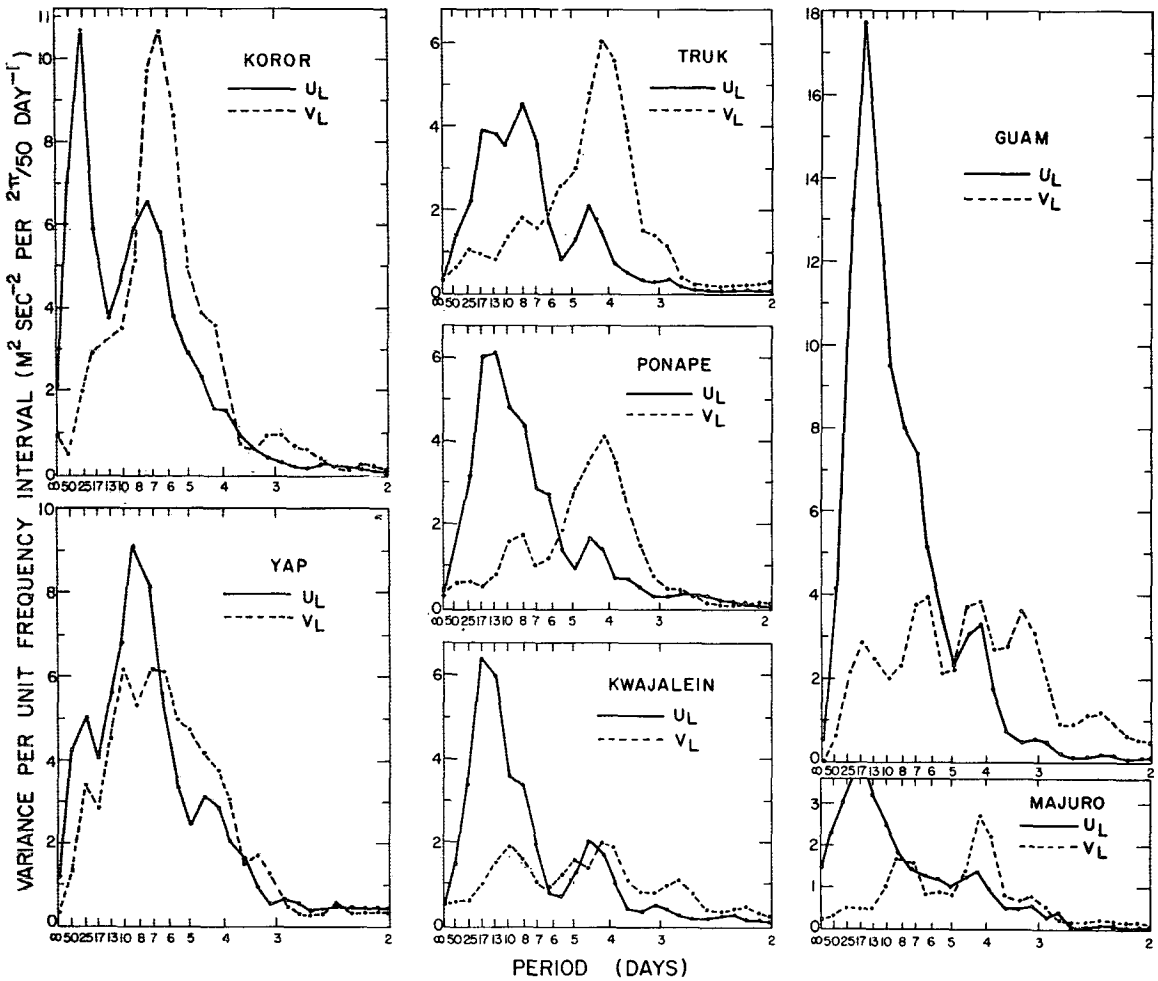

FIG. 1. Power spectra for the vertically averaged (surface–400 mb) zonal and meridional wind components at selected stations.

wind fluctuations are increasing with height; T_2, ~300 mb where the wind fluctuations undergo the phase reversal; and T_3, ~125 mb where the amplitude is decreasing with height. The gradient wind relationship suggests that each of these layers should be marked by distinct temperature fluctuations with phase reversals between adjacent layers. Relative humidity was averaged from the surface to 550 mb, as in (A).

The spectra for the zonal and meridional wind components in the lower layer, u_L and v_L, are shown in Fig. 1. The v_L spectra are characterized by a strong peak which occurs ~4 5 days at all stations except Koror and Yap, where it falls closer to 6 days. The magnitude of the peak in v_L is more pronounced at the lower latitude stations and increases westward. It is much larger at all stations than was observed in the previous year (A). The u_L spectra show evidence of a small related peak but most of the power is found at lower frequencies, as was the case the previous year. The amplification of the waves and the shift toward lower frequency may be a reflection of the changing vertical profile of mean zonal wind which the waves encounter as they move westward through the network (see Fig. 2).

Figs. 3a and b show spectral density of zonal and meridional wind components as a function of height at Truk. From this figure it is apparent that the upper troposphere is characterized by high spectral density

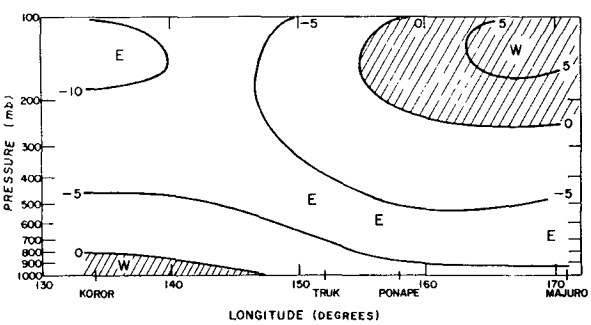

FIG. 2. Zonal cross section of mean zonal winds near 8N. Westerlies are shaded.

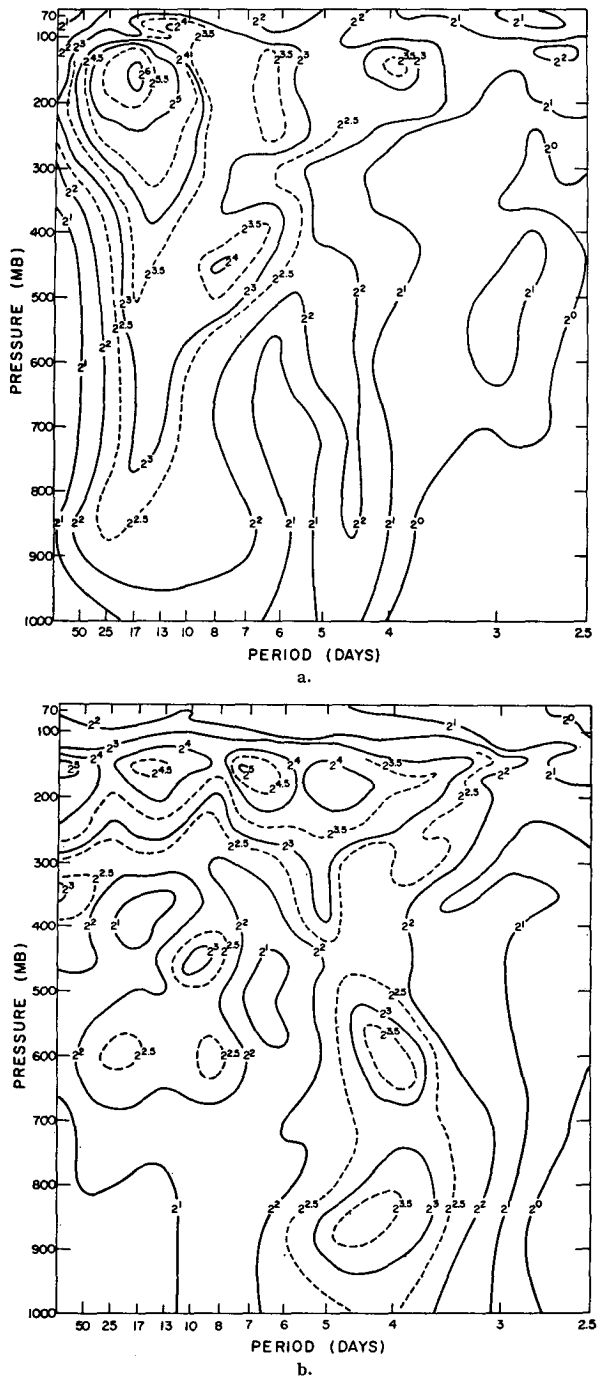

FIG. 3. Vertical distribution of power spectral density for the zonal wind component at Truk (plotted in powers of 2), a., and for the meridional wind component, b.

with a rather complex frequency distribution, as compared to the single distinct power peaks found in the lower tropospheric spectra. There is still considerable power in the meridional component at the 4–5 day period. However, this is overshadowed by a stronger peak in the vicinity of a week at most stations. Most of the variance associated with the u component is confined to low frequencies.

The power spectra were computed for T_1, T_2 and T_3 at all stations but the results are omitted for the sake of brevity. In general, the spectra were close to the noise level as was the case the previous year (A). There was some tendency for peaking near 4–5 days particularly in the case of T_1. The relative humidity ($\overline{\text{RH}}$) spectra all showed peaks at periods close to those encountered in the v_L spectra. Fig. 4 shows a composite $\overline{\text{RH}}$ spectrum for those stations which had 4–5 day peaks in v_L. A peak near 4–5 days is evident.

b. Vertical structure of the waves

The cross spectra between the various vertically averaged quantities were computed at each station. The program was run with a $6\frac{1}{2}$ day lag period (13 data points). This produced spectral estimates with $\sim$26 degrees of freedom. Coherence squares ≥ 0.11 are significant at the 95% level. The results for the 0.24 cycle day^{-1} frequency band (0.18 at Koror and Yap) are shown in Table 4.

Cross spectra between v_L and v_H have significant coherence and are $> \frac{1}{3}$ of a cycle out of phase at Ponape, Truk, Koror and Yap, and in phase at Kwajalein. The coherence square is not significant at Majuro. These results are in agreement with the interlevel phase and coherence data in Table 2.

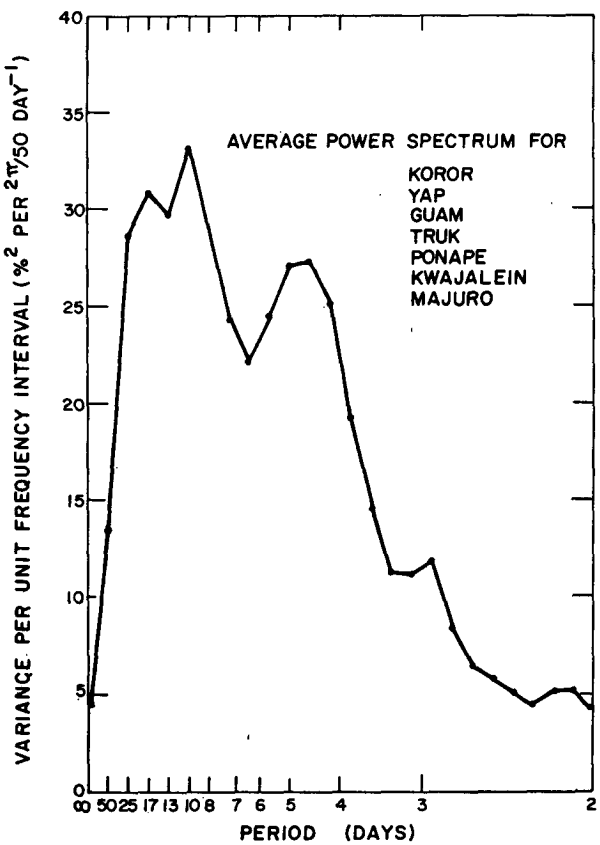

FIG. 4. Composite spectrum of vertically averaged (surface–550 mb) relative humidity.

TABLE 4. Inter-parameter cross-spectra results for the 0.24 cycle day^{-1} frequency band.

a. Coherence square.

(Significance level $\geq$95% if coherence^2 $\geq$0.11).

Coherence^2

Station	v_H	Base series: v_L u_L	T_1	T_2	$\overline{RH}$	Base series: T_2 T_1	T_3	$\overline{RH}$
Majuro	0.02	0.16	0.20	0.12	0.22	0.11	0.11	0.35
Kwajalein	0.21	0.22	0.17	0.02	0.19	0.03	0.17	0.03
Ponape	0.14	0.09	0.42	0.17	0.48	0.08	0.04	0.12
Truk	0.24	0.24	0.25	0.15	0.47	0.04	0.35	0.11
Guam	0.07	0.24	0.23	0.08	0.37	0.04	0.29	0.08
Yap*	0.29	0.07	0.19	0.23	0.17	0.21	0.08	0.22
Koror*	0.25	0.19	0.19	0.48	0.15	0.15	0.06	0.18

* 0.18 cycle day^{-1} frequency band.

b. Phase difference (in cycles).

(Positive values indicate that the base series leads the other series.)

Phase

Station	v_H	Base series: v_L u_L	T_1	T_2	$\overline{RH}$	Base series: T_2 T_1	T_3	$\overline{RH}$
Majuro		−0.05	0.34	−0.43	−0.22	−0.41	0.39	0.08
Kwajalein	−0.03	−0.06	0.44	--	0.00	—	0.48	—
Ponape	−0.35	—	0.25	−0.17	−0.30	—	—	−0.09
Truk	−0.41	0.00	0.33	−0.27	−0.23	—	0.50	0.01
Guam	—	0.08	0.48	—	−0.10	—	0.48	—
Yap*	−0.35		0.30	−0.16	−0.22	−0.45	—	0.05
Koror*	−0.42	0.07	0.41	−0.13	−0.09	−0.42	—	−0.01

* 0.18 cycle day^{-1} frequency band.

The spectra between v_L and u_L show marginally significant coherence and are in phase in this frequency range. This is in agreement with the results for the previous autumn (A) and for the spring of 1962 (Nitta, 1970).

Table 4 shows that v_L leads T_1 by 0.25–0.45 cycle and lags T_2 by 0.13–0.43 cycle. This supports the model inferred from the wind data on the basis of the gradient wind relation. The troughs of the waves are cold at low levels, but are surmounted by a region of warm temperature anomalies. The tendency for an out-of-phase relationship between T_2 and T_1 confirms this picture. There appears to be another temperature reversal between the layers represented by T_3 and T_2 at the stations where the coherence squares are high enough to be significant. This is also consistent with the gradient wind relation.

Relative humidity shows strong coherence with v_L, even at the eastern stations where the waves are relatively weak. The phase relation given in Table 4 places the most humid region slightly east of the trough in the streamline pattern, in agreement with the results for the previous autumn (A). The phase relation varies somewhat from station to station, but there is no indication of a systematic trend with longitude.

Dynamical models of easterly waves in which vorticity advection is the controlling influence on the vertical motion field place the region of maximum upward motion $\frac{1}{4}$ of a cycle east of the trough, or in phase with v_L (e.g., see Krishnamurti and Baumhefner, 1966; Yanai and Nitta, 1967). This is in contrast to large-amplitude tropical systems in which frictional convergence in the planetary boundary layer is the determining factor. In such systems there should be a strong positive correlation between upward motion and the vorticity of the low-level wind field. Recent analyses of the wind field at the low cloud level (e.g., Fujita *et al.*, 1969) suggest that this relationship holds for a wide variety of tropical disturbance types. For a westward propagating wave imbedded in an easterly current this would imply maximum upward motion in the troughs, or $\frac{1}{4}$ of a cycle in advance of the maximum v_L. If $\overline{RH}$ can be taken as an indicator of vertical motion, the phase relationships observed in the present study place the maximum upward motion between the two values mentioned above. This suggests that both influences are important.

An in-phase relationship between T_2 and $\overline{RH}$ is apparent at most stations. If we can assume that $\overline{RH}$ maxima are associated with convective activity, it follows that the middle troposphere is warmest at the times when latent heat is being released. The implications of this relationship are discussed more fully in Section 4.

c. Horizontal wavelength

Interstation cross spectra were computed for v_L, v_H and the meridional wind component at 80 mb, again with 13 lags. The results for the 0.24 cycle day^{-1} frequency band are shown in Fig. 5. In all three cases the waves are westward propagating. In both tropospheric layers the wavelength is close to 4000 km, while at 80 mb a wavelength of ~8000 km is indicated.

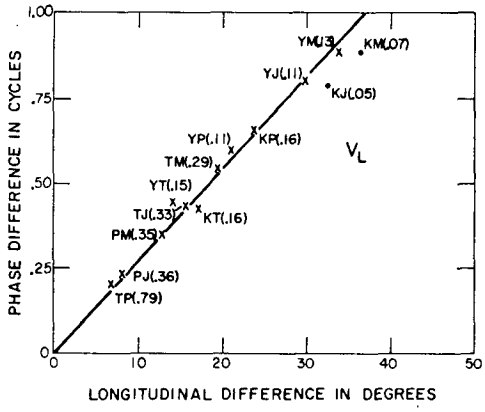

FIG. 5a. Phase difference in cycles between the meridional wind fluctuations in the 0.24 frequency band as a function of longitude difference between stations. Computations are based on the vertically averaged series v_L (surface–400 mb). Each data point is labelled with the identifiers of the pair of stations involved. Longitude difference is measured from the first station eastward to the second station. Phase difference is plotted as the amount by which the fluctuations at the first lag those at the second. Coherence squares are plotted beside the data points. Crosses denote coherence squares ≥ 0.11 which is the 95% significant level.

The lower tropospheric value is in close agreement with that computed for easterly waves during the previous autumn (A) and with the value deduced from satellite photographs for the summer of 1967 (Chang, 1970), while the stratospheric value is in accord with estimates by Yanai *et al.* (1968) for the mixed Rossby-gravity mode at the 17-km level.

It should be noted that Canton Island was not included in the above phase computations, its latitude being incompatible with those of the other stations. Recently, Nitta (1970) showed evidence that the disturbances with strong phase tilt in the lower troposphere (which seem to be characteristic of Canton Island and stations further east in the Pacific) have wavelengths closer to 8000 km. For these disturbances Nitta found that the wavelength is the same in the troposphere and stratosphere, and there is evidence of significant coherence between the waves in the two regions. Our interlevel coherences for Canton Island (Table 2) support this viewpoint. Unfortunately, the stations available to us did not allow us to verify Nitta's wavelength computations for the eastern stations.

4. Discussion and conclusions

July–December 1964 was marked by strong oscillations in the meridional wind component at lower tropospheric levels, with periods ranging from 4–5 days at the eastern stations to 6–7 days in the extreme western Pacific. The amplitudes increased from ~3 m sec^{-1} at Majuro to ~8 m sec^{-1} at Koror. The variance in this frequency range was almost an order of magnitude larger than during the previous year.

The waves observed at Canton Island exhibit the same phase inclination with height as those studied previously by Yanai *et al.* (1968) and Nitta (1970). Nitta has suggested that these may be the tropospheric manifestation of the mixed Rossby-gravity mode, first identified at stratospheric levels by Yanai and Maruyama (1966). These waves were not present at Canton Island a year earlier (A).

Further west in the Pacific the tropospheric disturbances were clearly distinct from the mixed Rossby-gravity mode in the lower stratosphere, as evidenced by their shorter wavelengths (4000 km as opposed to 8000 km) and their lack of coherence with the latter. These waves were marked by a relative absence of phase inclination with height. The observed phase relationships between wind, temperature and relative humidity at various levels in these waves (Tables 2 and 4) are illustrated schematically in Fig. 6. (It is assumed that high relative humidity is indicative of strong convective activity.) These relationships suggest the following possible interpretations of the energetics of these disturbances:

1) Regions of strongest convective activity are cooler than their surroundings at the surface and warmer than their surroundings in the vicinity of the 300-mb level.

2) The coincidence of warmest temperatures at ~300 mb with the region of strongest convection implies that the release of latent heat tends to enhance the horizontal temperature gradients at this level, thus serving as a source of available potential energy for the waves.

3) The phase relationship between v_L and $\overline{RH}$ suggests low-level inflow into troughs, where convection is occurring, and high-level outflow from the ridges. This cross-isobar flow toward lower pressure implies a conversion from available potential to kinetic energy in the waves. This is essentially the same mechanism as proposed by Riehl (1959).

4) The concept of conditional instability of the second kind, as discussed by Charney and Eliassen (1964) and Kuo (1965) for symmetric vortices, may be applicable to these disturbances.

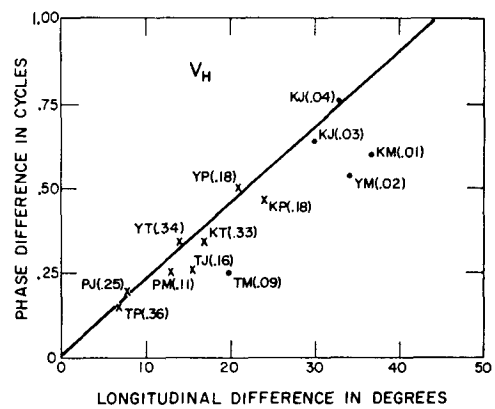

FIG. 5b. Same as Fig. 5a except for the vertically averaged series v_H (200–125 mb).

Despite the above evidence in favor of latent heat as an energy source, we cannot completely discount the possibility that barotropic instability may also play a role in the energetics of these disturbances. The in-phase relationship between u and v at the lower levels (Table 4) is indicative of a northward flux of westerly momentum across the ITCZ. This flux is directed down the gradient of mean zonal wind, i.e., from the equatorial westerlies (or light easterlies) into the trades. Thus, there is, in this region, a conversion from zonal to eddy kinetic energy. Further studies will be needed to determine the relative magnitudes of the energy conversions taking place in these waves.

In view of the qualitative similarity of the structure of the observed waves at the western stations and that of incipient tropical storms, it might be questioned whether the observed waves were merely the reflection of the passage of typhoons or pre-typhoon depressions through the network. It is clear that this was not the case. Out of ~30 waves which passed through the network during the period of investigation, only five could be identified with tropical storm or typhoon developments while in the vicinity of or slightly west of Truk. A few more may have been associated with storm developments which took place to the north of the network. Thus, it is apparent that most of these disturbances maintain their identity as westward propagating waves of moderate intensity, rather than transforming into symmetric vortices.

Nevertheless, there is evidence that the number of typhoon developments in a given year may depend upon the relative intensity of the wave activity in this frequency range. For example, the unusual strength of the waves during the 1964 season appears to be reflected in the typhoon statistics (U. S. Department of Commerce, 1962 68). The year 1963 had a total of 26 typhoons and tropical storms of which only three formed between 5 and 10N. This is more or less typical of the data for the past five years. By way of contrast, the year 1964 was marked by 44 storms, of which 14 formed between 5 and 10N.

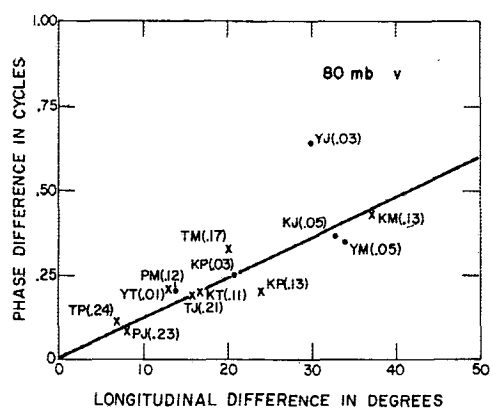

FIG. 5c. Same as Fig. 5a except for the series v at 80 mb.

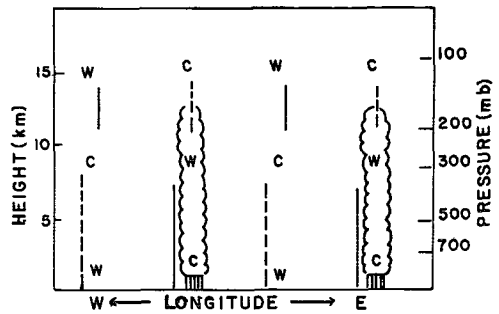

FIG. 6. Schematic zonal cross section through the observed wave disturbances in the western Pacific. Heavy solid and dashed lines represent trough and ridge position, respectively. The letters C and W denote temperature anomalies. The clouds sketched in the figure represent the positions of maximum convective activity.

Acknowledgments The authors wish to thank Drs. Richard J. Reed and James R. Holton for their interest and suggestions. Data for the study were provided by the U. S. Navy Weather Research Facility. This work was supported by the National Science Foundation under Grants GA-629X and GA-629X2.

REFERENCES

Amos, D. E., and L. H. Koopmans, 1963: Tables of the distribution of the coefficient of coherence for stationary bivariate Gaussian processes. Sandia Corp., Albuquerque, N. M., Mono. SCR-483.

Chang, C.-P., 1970: Westward propagating cloud patterns in the tropical Pacific as seen from time-composite satellite photographs. *J. Atmos. Sci.*, **27**, 133–138.

Charney, J. G., and A. Eliassen, 1964: On the growth of the hurricane depression. *J. Atmos. Sci.*, **21**, 68–75.

Fujita, T., K. Watanabe, and T. Izawa, 1969: Formation and structure of equatorial anticyclones caused by large scale cross-equatorial flows determined by ATS-1 photographs. *J. Appl. Meteor.*, **8**, 649–667.

Kuo, H. L. 1965: On formation and intensification of tropical cyclones through latent heat release by cumulus convection. *J. Atmos. Sci.*, **22**, 40–63.

Krishnamurti, T. N., and D. Baumhefner, 1966: Structure of a tropical disturbance based on solutions of a multilevel baroclinic model. *J. Appl. Meteor.*, **5**, 396–406.

Nitta, T., 1970: Statistical study of tropospheric wave disturbances in the tropical Pacific region. *J. Meteor. Soc. Japan*, **48** (in press).

Riehl, H., 1959: On the production of kinetic energy from condensation heating. *The Atmosphere and Sea in Motion*, New York, Rockefeller Press, 381–399.

U. S. Department of Commerce, 1962–1968: Climatological data —National summary. Vols. 12–18.

Wallace, J. M., and C.-P. Chang, 1969: Spectrum analysis of large-scale wave disturbances in the tropical lower troposphere. *J. Atmos. Sci.*, **26**, 1010–1025.

Yanai, M., and T. Maruyama, 1966: Stratospheric wave disturbances propagating over the equatorial Pacific. *J. Meteor. Soc. Japan*, **44**, 291–294.

——, and T. Nitta, 1967: Computation of vertical motion and vorticity budget in a Caribbean easterly wave. *J. Meteor. Soc. Japan*, **45**, 444–466.

——, T. Maruyama, T. Nitta and Y. Hayashi, 1968: Power spectra of large scale disturbances over the tropical Pacific. *J. Meteor. Soc. Japan*, **46**, 308–323.